The ROYAL COLLEGE of OPHTHALMOLOGISTS

www.nature.com/eye

ARTICLE

Check for updates

Two potentially distinct pathways to geographic atrophy in age-related macular degeneration characterized by quantitative fundus autofluorescence

Wei Wei[1,2], Marco Mazzola[1,3], Oscar Otero-Marquez[1], Yuehong Tong[1], Eric Souied[4], Giuseppe Querques[5], K. Bailey Freund[6] and R. Theodore Smith[1]✉

BACKGROUND/AIMS: To demonstrate two distinct pathways to geographic atrophy (GA) that originate from soft drusen/ pigment epithelial detachments (PEDs) and subretinal drusenoid deposits (SDDs), respectively, and are characterized by their final quantitative autofluorescence (qAF) levels.

METHODS: 23 eyes of 18 patients with GA underwent spectral-domain optical coherence tomography (SD-OCT) and qAF imaging on the qAF-ready Heidelberg Spectralis. 52 GA Regions-of-interest (ROIs), or clusters of adjacent lesions, were selected, and the ROIs were divided into groups by the dominant iAMD precursors on prior serial tracked SD-OCT scans. Mean qAF values and structural SD-OCT findings of groups were compared.

RESULTS: Group 1 lesions (soft drusen/PED precursors, 18/52) were isolated, with lower mean qAF (35.88 ± 12.75 units); group 3 lesions (SDD precursors, 12/52) were multilobular, with significantly higher mean qAF (71.62 ± 12.12 units, $p < 0.05$). Group 2 lesions, (mixed precursors, 22/52) had intermediate mean qAF (58.13 ± 67.92 units). Significantly greater prevalence of split RPE/ Bruch's membrane complex in SDD-associated GA, suggesting basal laminar deposit (BLamD), than in drusen-associated lesions was the major structural difference.

CONCLUSION: Quantitative autofluorescence (qAF) of GA lesions may reflect two distinct pathogenic pathways and structural outcomes, originating from soft drusen/PED and subretinal drusenoid deposits (SDDs), with the final qAF values lower or higher, respectively. Basal laminar deposit specifically in and adjacent to SDD-associated lesions may account for their greater autofluorescence. The potential importance of this paradigm is that it could direct, simplify and facilitate research on geographic atrophy by dividing the disease into two components that may be studied separately.

Eye (2023) 37:2281–2288; https://doi.org/10.1038/s41433-022-02332-8

INTRODUCTION

The mechanism of geographic atrophy (GA) in age-related macular degeneration (AMD) is unknown, and its anatomy by spectral-domain optical coherence tomography (SD-OCT) is complex [1]. The principal precursor lesions of GA are the two distinct lesions of intermediate AMD (iAMD): soft drusen, beneath, and subretinal drusenoid deposits (SDD) above, the retinal pigmented epithelium (RPE) [2]. Both soft drusen and SDD, also called reticular pseudodrusen (RPD) [3], are risks for both the exudative and atrophic late forms of AMD, and SDDs confer twice the risk [4–6]. Other distinguishing features between these lesions are the associations of SDD with type 3 macular neovascularization [7] and the *ARMS2* risk allele [8].

Fundus autofluorescence (AF), which normally images primarily the lipofuscin of the RPE, is a powerful indicator and classifier of outer retinal pathology. Sub-RPE fluorophores detected in AMD include soft drusen, basal linear deposit (BlinD) and basal laminar deposit (BLamD) [9]. AF can reliably identify the RPE loss in GA by the marked loss of RPE autofluorescence [10, 11]. However, residual AF from sub-RPE fluorophores can remain. Indeed, AF levels in GA are not uniform, with certain lesions appearing "gray" and others "dark". Fleckenstein et al. [12] demonstrated gray GA lesions in the diffuse tricking AF phenotype with splits of the RPE/Bruch's membrane (BrM) complex in the GA border zone on SD-OCT. The thick RPE band was posited to contain BLamD, thus explaining the stronger AF. This GA phenotype also has high SDD loads and strong associations with systemic vascular disease [13].

Mones et al. further classified eyes with GA into three clusters based on the qualitative appearance of the GA lesions (light or dark) in the eye and the eye's predominant iAMD lesion (soft drusen, mixed drusen and SDD, or SDD) [14]. They found that eyes with soft drusen and dark GA clustered together, as did eyes with SDD and light GA, with a third mixed group with drusen, SDD and mixed GA lesions. Classification was performed on a per eye basis. Individual GA lesions or regions of interest (ROIs) were not considered, and no explanation for their appearance was

[1]Ophthalmology, Icahn School of Medicine at Mount Sinai, New York, NY, USA. [2]Ophthalmology, The Second Xiangya Hospital, Central South University, Changsha, Hunan, China. [3]Ophthalmology, University of Insubria Varese-Como, Viale Luigi Borri, Varese, Italy. [4]Department of Ophthalmology, Hôpital Intercommunal de Créteil Université, Créteil, France. [5]Ophthalmology, University Vita-Salute, Via Olgettina, Milan, Italy. [6]Vitreous Retina Macula Consultants of New York, New York, NY, USA. ✉email: rts1md@gmail.com

Received: 16 March 2022 Revised: 18 October 2022 Accepted: 24 November 2022
Published online: 9 January 2023

proposed. This construct was later modified into 3 different groups of GA eyes with inclusion of genetics, but without AF imaging [15].

We propose that the descriptions by Mones and Fleckenstein of GA as "dark" or "gray" on AF could be usefully sharpened in several ways with the technique of quantitative autofluorescence (qAF) [16]. By employing a fixed internal fluorescent reference to account for variable laser power and detector sensitivity [16], qAF provides reproducible quantification and comparison of the AF intensity of the fundus between patients and across time [17]. Thus, we can objectively stratify individual GA lesions, rather than eyes, by their mean qAF levels, and further, by examining time series of previous, registered SD-OCT scans, can determine the iAMD origins and pathways (from drusen or SDD) to each GA lesion. This will allow correlation of GA qAF with predecessor lesions. Further, by considering lesions rather than entire eyes, we propose a simple construct in which there are two distinct pathways to GA, from the two known major precursors, drusen and SDD, which may present separately or in combination in a given eye. These two pathways could be considered individually as a strategy to better interpret research on GA mechanisms, treatments and prognostic factors for disease progression. Finally, by comparing SDD-associated GA to drusen-associated, we will search for the source of the greater qAF, or "gray" appearance, of the former.

METHODS

Patients

This cross-sectional study was conducted at the Vitreous-Retina-Macula Consultants of New York (VRM) and New York Eye & Ear Infirmary of Mount Sinai (NYEEI). Inclusion criteria were: age older than 60 years, diagnosis of AMD with GA and no exudation in study eye, pseudophakia with clear posterior capsule of the study eye, and AF and tracked SD-OCT images over at least 1 year previously on the Heidelberg Spectralis HRA + OCT (Heidelberg Engineering, Franklin, MA) with automated retinal tracking (8–16) and quality (29–34), per Spectralis specifications. If both eyes met study criteria, both eyes were enrolled. Exclusion criteria included: prior intravitreal injection, retinal vascular disease such as diabetic retinopathy, other retinal degeneration or surgery, or epiretinal membrane interfering with imaging. The study protocol adhered to the tenets of human research in the Declaration of Helsinki and was approved by both the Institutional Review Board (IRB) at NYEEI and the Western IRB (Puyallup, WA) for VRM. A written informed consent was obtained from each subject.

Study design

Patients had dilated exams of both eyes, color fundus photography (CFP), near-infrared reflectance (NIR-R), AF, qAF, and SD-OCT imaging. Medical, family, and social history were reviewed by questionnaire (Table 1).

Image acquisition

NIR-R, AF, qAF, and SD-OCT images (Figs. 1, 2) were acquired on the qAF-ready Spectralis in follow-up mode, in registration with prior exams. The media spectral transmission correction factor was set to default (age = 21) because all patients were pseudophakic. 12 successive images were recorded (30° field of view, 768 × 768 pixels). Images with inhomogeneous illumination (versus the normally inhomogeneous AF pattern and that due to pathology), sectoral opacities or unstable fixation were excluded. A mean of at least nine was then calibrated to the embedded reference (HEYEX; version 1.9.10.0) to yield the qAF image [16]. CFP was performed with the Topcon-50DX (Topcon Medical Systems, Oakland, NJ). The SD-OCT protocol comprised 20° horizontal raster line scans centered over the macula, 20° in vertical extent, numbering 19 to 49 B-scans of the specified quality.

qAF image analysis

ROIs were selected from the GA lesions in the qAF scans. The ROIs were either individual GA lobules (Fig. 1C) or grouped coalescent lobules of fairly uniformly decreased AF (Fig. 2C). They were outlined manually by one grader (WW) with the "QAF region", a highly consistent method [10, 11].

Table 1. Demographic and clinical characteristics of the study population.

Characteristic	Category	*n*	%
Sex	Male	3	16.7
	Female	15	83.3
Age (Years)	68–70	1	5.6
	71–80	4	22.2
	81–90	9	50
	91–94	4	22.2
Family history of AMD	Yes	5	27.8
	No	13	72.2
Smoking	Current	1	5.6
	No	12	66.7
	Former	5	27.7
Hypertension	Yes	11	61.1
	No	7	38.9
Hyperlipidaemia	Yes	12	66.7
	No	6	33.3
CNV in fellow eye	Yes	7	38.9
	No	11	61.1
Kidney failure	Yes	2	11.1
	No	16	88.9
Coronary artery disease	Yes	4	22.2
	No	14	77.8

The minimum diameter for inclusion was 250 microns. Peripapillary atrophy was excluded. Mean qAF of the ROIs in qAF units and their areas were measured by the HEYEX software and displayed (Figs. 1 and 2).

Image tracking for ROI classification

We traced the individual ROIs in prior serial eye-tracked SD-OCT scans back to their iAMD baseline lesions and divided them into three groups. Group 1 ROIs had soft drusen/PED precursors, group 2 ROIs had mixed drusen and SDD precursors, and group 3 ROIs, SDD precursors. Some eyes had ROIs in multiple groups. To be judged as having SDD, an ROI had to show five or more SDDs by near-infrared and SD-OCT imaging. Two readers (WW, RTS), blinded to subsequent qAF outcomes, independently performed this categorization and openly resolved any disagreements. SD-OCTs and qAF measures from group 1 and group 3 ROIs are illustrated (Figs. 1 and 2).

Structural data from Final SD-OCT scans

Any atrophy within the ETDRS circle of 500 micrometer radius [18] was classified as "foveal", or was otherwise "extrafoveal". We examined all B-scans that traversed the ROIs for the presence within GA or its 500-micrometer border zone of Basal Laminar Deposit (BLamD) in the form of RPE plateaus and/or split RPE/Bruch's Membrane (BrM) complexes (Figs. 2, 3) [19]. For each eye, we chose one ROI for analysis, to avoid multiple samplings, and we chose the largest, regardless of the group it represented, to maximize the total number of B-scans passing through it. Each of these scans was inspected in the ROI and border zone for presence of those structures consistent with BLamD. The ratio of the number of scans with any BLamD to the total number of scans through each ROI was recorded. Scans through SDD-associated GA were also reviewed for the presence of any retained RPE in the GA that may have additionally contributed to the AF.

qAF images were exported to Adobe Photoshop (Version 13.0.1; Adobe Systems Inc, San Jose, CA) for further analysis. Serial multimodal imaging of an eye with both drusen and SDD precursors progressing to two characteristic GA ROIs is shown in Fig. 3.

To evaluate the health of the RPE outside the GA, we recorded mean qAF over all eyes from the totality of GA lesions, and from the remainder of the macula in the standard 6000 micrometer diameter central grading circle.

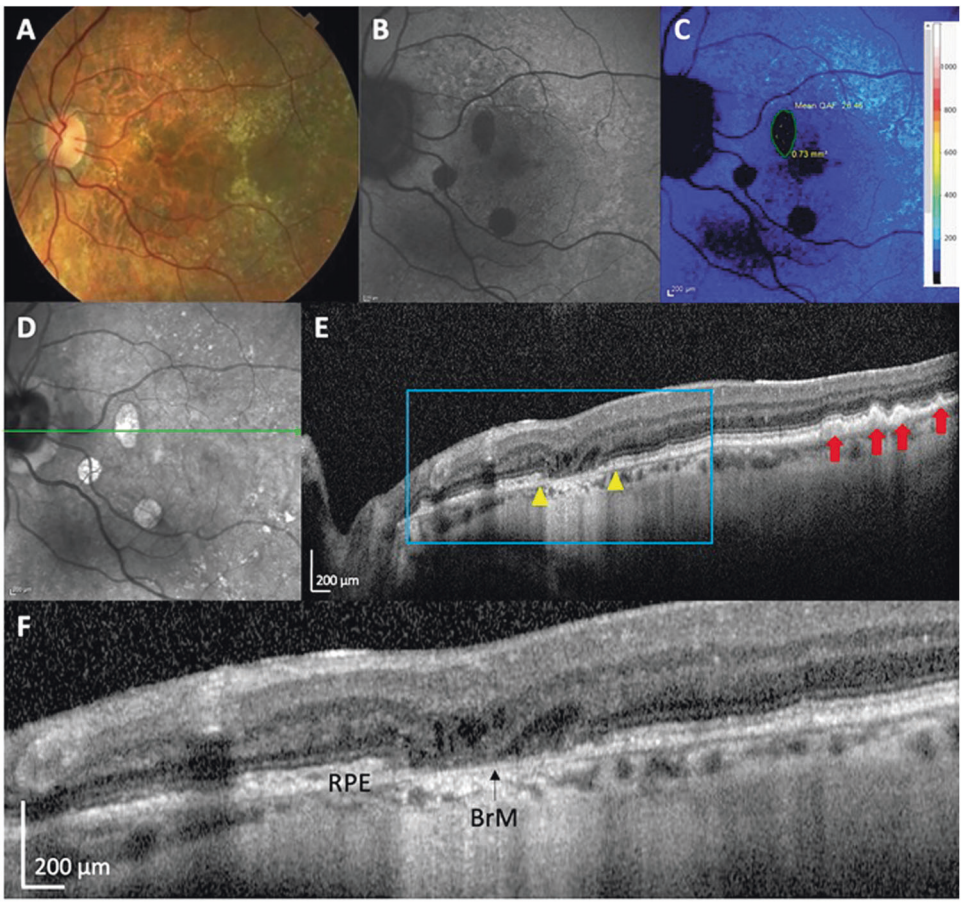

Fig. 1 Quantitative autofluorescence (qAF) of Geographic Atrophy (GA) with soft drusen precursors. A Color fundus photograph, shows generalized retinal pigment epithelial (RPE) thinning, scattered drusen peripherally. **B** Autofluorescence (AF) image. Three "dark" hypoautofluorescent (hypoAF) lesions suggest GA. **C** Quantitative fundus AF (qAF) image. One hypoAF lesion outlined in yellow was chosen as region-of interest (ROI), mean qAF, 26.46 qAF units; GA area, 0.73 mm^2. qAF is coded to the color bar in qAF units. **D** NIR image. GA lesions are hyperreflectant. Green line shows horizontal axis and extent of the SD-OCT scan. **E** SD-OCT scan. There is complete RPE and outer retinal atrophy (cRORA), with choroidal hypertransmission, absence of the RPE band and thinning of the overlying retina (bounded by yellow arrowheads). Soft drusen appear as hyperreflective mounds between the RPE and Bruch's membrane (BrM) (red arrows). Blue box demarcates inset, **F** Magnified inset. cRORA is better visualized. BrM is visible as a thin hyperrflective band, with remaining RPE on either side. There is no evidence of basal laminar deposit in the form of RPE plateaus and/or split RPE/BrM complex.

Subfoveal choroidal thickness (SFCT) in microns from the outer limit of the RPE to the inner surface of the sclera was measured independently on the same scan by two investigators using the built-in callipers and the mean was calculated. All data were exported to Excel (Microsoft Excel 2016, version 15.14; Microsoft Corporation, Redmond, WA).

Statistical analysis

Power calculations relied on [14], which found AF differences ($p < 0.013$) between three groups of ~ 25 eyes. We studied individual ROIs as the test set, based on our hypothesis that disease pathways and qAF levels are connected in individual ROIs. Hence, three groups of 18 ROIs would yield 80% power to detect different qAF levels, $p = 0.05$. 54 ROIs total, divided into three groups by their iAMD precursors, would power the study adequately.

Continuous SFCT and qAF data were analysed with the Kolmogorov–Smirnov (K–S) test for normality and group means compared by the unpaired *t*-test. Non-normally distributed data were analysed with the Kruskal–Wallis non-parametric test. A *p* value less than 0.05 was accepted as statistically significant.

RESULTS

Clinical characteristics

We analysed 23 eyes of 18 subjects, mean age 85 ± 6.5 years. with 52 ROIs of GA. Mean follow-up time was 5.5 years (range 1.2~10). Clinical characteristics are summarized in Table 1. By eye, at baseline, phenotypes were soft drusen/PED in 8 eyes and SDD in 5 eyes; the other 10 of 23 eyes had mixed soft drusen/PED and SDD. As has been observed, soft drusen/PED tended to be found centrally and SDD more peripherally (Table 2. Figs. 1, 2, 3) [14]. In the mixed eyes, this pattern was maintained, with overlapping drusen/SDD phenotypes found at the borders of more pure phenotypes (Fig. 3, B2). At baseline, the mean SFCT of the soft drusen eyes was 227.87 ± 38.14 µm, of the mixed eyes, 205.55 ± 73.63 µm, and of the SDD eyes, 167.19 ± 49.57 µm. The data were normally distributed by the K–S test. The SFCT in eyes with SDD was significantly thinner than the eyes with soft drusen (*t*-test, $p < 0.05$). At last visit, the mean SFCT of the soft drusen eyes was 182.62 ± 38.89 µm, of the mixed group, 171.77 ± 79.32 µm, and of the SDD group, 147.66 ± 53.99 µm, not significantly different.

GA regions of interest (ROIs). Characteristics and progression

18 ROIs were assigned to group 1 (soft drusen/PED precursors), 22 ROIs to group 2 (mixed soft drusen and SDD precursors), and 12 ROIs to group 3 (SDD precursors). ROIs in group 1 were characterized by foveal atrophy and isolated lesions, and ROIs in group 3 by extrafoveal atrophy and multilobular lesions. (Table 2).

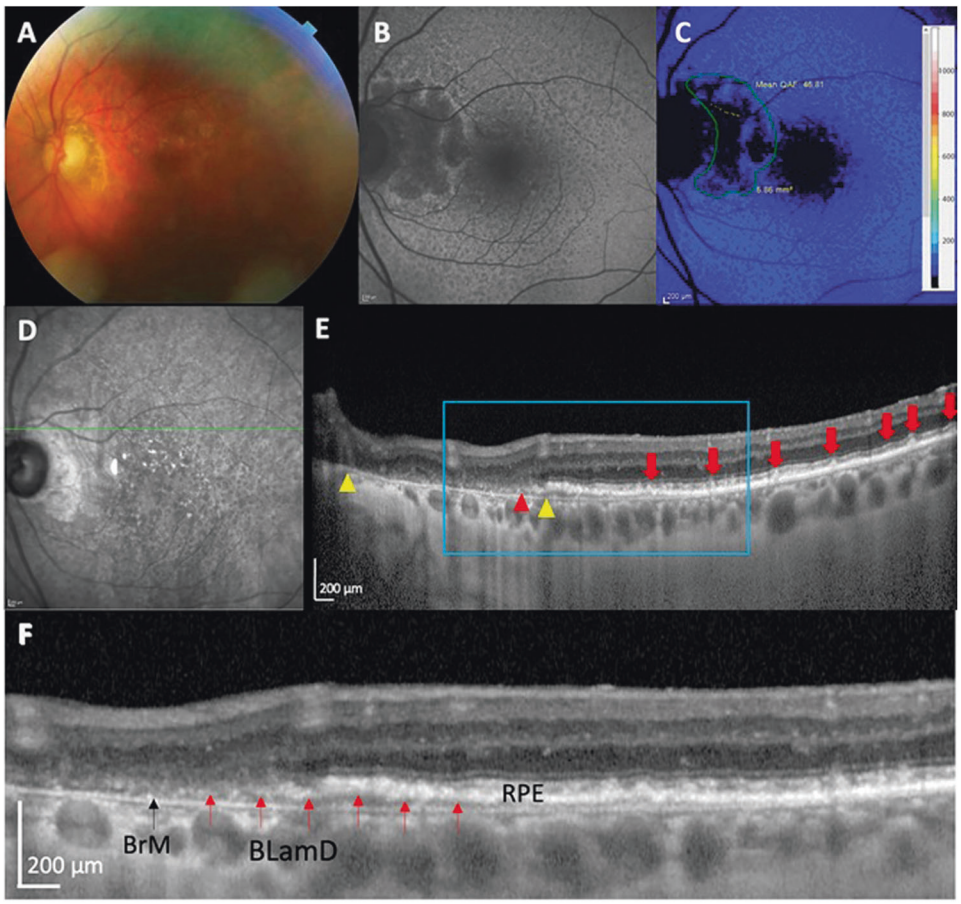

Fig. 2 Quantitative autofluorescence (qAF) of Geographic Atrophy (GA) with subretinal drusenoid deposit (SDD) precursors and basal laminar deposit (BLamD). A Color fundus photograph (CFP) shows GA adjacent to peripapillary atrophy. **B** Autofluorescence (AF) image shows "gray" hypoAF lesion with lobed edges corresponding to the GA in the CFP. HypoAF dots corresponding to SDD are confluent in the macula. **C** Quantitative fundus autofluorescence (qAF) image. Region-of interest (ROI), outlined in yellow; mean qAF, 46.81 qAF units; GA area, 5.86 mm². Peripapillary atrophy was not included. qAF is coded to the color bar in qAF units. **D** NIR image. The horizontal axis and extent of the SD-OCT scan through the ROI is indicated by the green line. **E** SD-OCT scan illustrates the features of incomplete retinal pigment epithelium (RPE) and outer retinal atrophy (iRORA), with alternating segments of preserved and degenerated photoreceptors, and one <50 micrometer segment of partially preserved RPE (red arrowhead) The extent of GA is delineated by yellow arrowheads. SDDs are visualized as hyperreflective material between RPE and ellipsoid zone (red arrows). Blue box demarcates inset (**F**) Magnified inset showing BLamD. Bruch's membrane is visible as a thin hyperreflective band. BLamD appears as a split RPE-BrM complex or "double-layer sign" at the right-hand red arrows and continuing temporally for ~1500 micrometers. The thick hyperreflective band is combined RPE and BlamD. There is a thin, speckled hyporeflective band separating it from BrM. Continuing along the left-hand red arrows, the RPE thins out with only BLamD remaining.

SDDs were dynamic structures that could increase in number (Fig. 3, A1–B1), grow to break through the ellipsoid zone (EZ) (Fig. 3, A1), or regress. Complete regression could be accompanied by either preservation of outer retina (Fig. 3, D1), outer retinal damage (Fig. 3, C1), if not complete outer retinal atrophy as has been described [10], or, with increasing damage, by progression to GA (Fig. 3, B1, C1, D1). Soft drusen were mostly already established at baseline, thus did not significantly increase in number, but often coalesced into drusenoid PED that then collapsed into atrophy (Fig. 3, B2, C2).

The mean areas of the ROIs in groups 1, 2 and 3, were $4.22 \pm 7.08\ mm^2$, $2.69 \pm 3.08\ mm^2$ and $2.72 \pm 2.57\ mm^2$, respectively, not significantly different.

qAF in GA and non-GA regions

The color-coded qAF images show both lower (darker blue) and higher (lighter blue) qAF levels (Figs. 1 and 2). The soft drusen/PED pathway produced mostly isolated and "black" GA lesions on AF, with lower qAF (Fig. 1). The SDD pathway produced mostly multifocal/coalescent and "gray" GA lesions on AF, with higher qAF (Fig. 2, Table 2). The qAF data were normally distributed (K–S test). The mean qAF was significantly higher in the SDD group (71.62 ± 12.12) than in the drusen group (35.88 ± 12.75, $p < 0.001$, t-test). The mean qAF of the mixed group was 58.13 ± 11.88, also significantly different from the soft drusen and SDD groups ($p < 0.05$, t-test). Considering only ROIs from right eyes, the mean qAF in the SDD group was 70.61 ± 13.04, and in the drusen group 35.86 ± 16.45, $p < 0.0001$. That of the mixed group was 58.30 ± 11.79, also significantly different from the other groups

The mean qAF of all GA regions combined was 66.65 ± 16.73, and of all non-GA regions, 99.92 ± 17.49, significantly higher ($p < 0.005$). However, non-GA regions had lower mean qAF values than historic, matched non-AMD controls (132.2 ± 42.8) [20].

Structural data from SD-OCT scans

The 23 ROIs from the 23 study eyes chosen for evaluation of BLamD numbered 8, 10, and 5 from the drusen, mixed and SDD groups, respectively. The total number of B-scans through these ROIs were 88, 122, 43. The percentages of scans through each

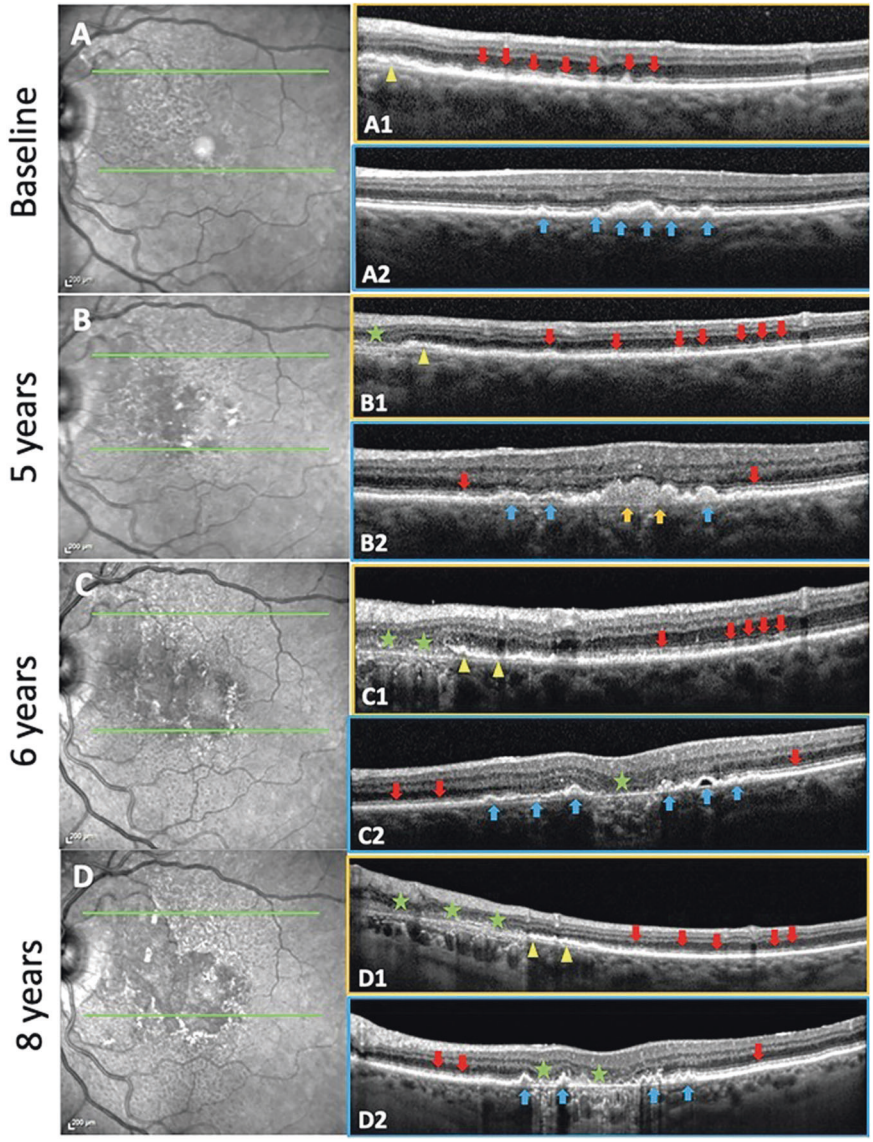

Fig. 3 Soft drusen and subretinal drusenoid deposits (SDDs) evolving and progressing to geographic atrophy (GA) in the same eye over 8 years with residual basal laminar deposit (BLamD) in a 79-year-old female. Left: NIR images. Right: SD-OCT B scans. Boxes outlined with orange, scans through an SDD region. Boxes outlined with blue, scans through a soft drusen region. **A** Baseline. NIR image. Hyporeflectant SDD are largely confined to the supero-nasal macula. Green lines in the NIR image show the horizontal axis and extent of two SD-OCT scans. **A1** The scan passes through a region with abundant SDD (red arrows), the next-to-last has broken through the ellipsoid zone, no drusen. Note the splitting of the RPE/BrM complex suggesting BLamD in the nasal aspect of the scan (yellow arrowhead). **A2** The scan passes through several large drusen and a pigment epithelial detachment (PED) (blue arrows), no SDD. No atrophy is seen in either scan. **B** 5-year follow-up. NIR image. SDD have expanded temporally and inferiorly. The SD-OCT scans are placed exactly as at baseline (green lines). **B1** There has been some flattening/resorption of former SDD, with new SDD appearing temporally (red arrows). A small area of GA has appeared nasally (green star), with no RPE and a thin line of BLamD, and a split RPE-BL-BrM complex is visible adjacent to the GA area (yellow arrowhead). No drusen. **B2** Here, there are adjacent lesions of both types. There has been growth and coalescence of soft drusen (blue arrows) into drusenoid PED (orange arrows). Minimal granular material and Stage 1 SDD have appeared temporally and nasally between the RPE and the ellipsoid zone (red arrows). No atrophy is seen in this scan. **C** 6-year follow up. NIR image. Confluent SDD can now be appreciated throughout almost all of the macula, including centrally where the NIR reflectance also shows other changes. SD-OCT scans placed as at baseline (green lines). **C1** The area of GA has extended temporally with no RPE and scattered BLamD (green stars), adjacent to a region of outer retinal damage and splitting of the RPE/BrM band characteristic of BLamD (yellow arrowheads). SDD temporally are less distinct (red arrows). No drusen. **C2** The large central drusenoid PED has collapsed into atrophy (green star), and the other predecessors seen in **A2** and **B2** have partially collapsed, with remaining soft drusen and PED (blue arrows). Subretinal granular material and Stage 1 SDD still present on either side (red arrows). **D** 8-year follow-up. NIR image. SDDs are now less apparent superonasally, where atrophy has supervened. SD-OCT scans, same placement (green lines). **D1** GA has expanded temporally, with no RPE and a thin line of BLamD (green stars), with further splitting temporally of RPE/BrM band into the SDD area (yellow arrowheads). SDD temporally have regressed almost completely, with preservation of the outer retina (red arrows). No drusen. **D2** There is new focal GA nasally and previous GA centrally (green stars) with intervening PEDs (blue arrows).

Table 2. Characteristics of geographic atrophy ROIs by predominant precursor lesions.

	Group 1 Soft drusen/ PED	Group 2 Mixed drusen / SDDs	Group 3 SDDs
Number of ROIs (*n*)	18	22	12
mean qAF ± SD (qAF units)	35.88 ± 12.75	58.13 ± 11.88	71.62 ± 12.12
Mean area ± SD (mm^2)	4.22 ± 7.08	2.69 ± 3.08	2.72 ± 2.57
GA aspect (%)			
•Isolated	61.11	54.54	33.33
•Multilobular	38.88	45.45	66.66
•Foveal	55.5	22.72	8.33
•Extrafoveal	45.5	77.27	91.66
ROIs examined for BLamD (*n*)	8	10	5
Number of B-scans through each individual ROI	7	7	7
	7	16	9
	6	14	7
	4	5	4
	7	10	16
	40	13	
	10	18	
	7	34	
		15	
		7	
% of scans for each ROI with BlamD*	0	43	100
	0	63	88
	0	7	57
	25	0	100
	0	10	56
	8	14	
	0	33	
	0	38	
		7	
		29	

BlamD basal laminar deposit, *PED* pigment epithelial detachment, *SDD* subretinal drusenoid deposit, *GA* Geographic atrophy, *ROI* region of interest, *qAF* quantitative autofluorescence, *SD* Standard deviation.
*Group ranks and all pairs of group ranks are significantly different (Kruskall–Wallis test).

ROI with BLamD were calculated (Table 2). The mean (median) percentages of scans with BLamD for each group were 4% (0%), 24% (22%), 80% (88%). The Kruskal–Wallis non parametric analysis of variance test for the difference between mean ranks of the 3 groups of individual percentages was significant ($p = 0.00079$). *Post hoc*, the differences between each pair of groups were also significant, $p = 0.006$, 0.002 and 0.013, for the pairs drusen::mixed, drusen::SDD, and mixed::SDD, respectively. We found only a few <50 micrometer segments of retained RPE, insufficient to shift mean qAF, in scans through SDD-associated GA (Fig. 2, SD-OCT scan, Fig. 3, B1, C1, D1, and discussions in legends)

DISCUSSION

Currently, there is no simple metric for evaluating lesions of GA that may be related to structure and pathogenesis. In this small study, the qAF of GA lesions was correlated to the predominant lesions of iAMD, soft drusen or subretinal drusenoid deposits (SDDs), that precede and evolve to them, with the qAF of those from SDD higher than those from soft drusen. Thus, it appears that qAF may be a marker for these important phenotypes. It also appears that the higher qAF in SDD-associated lesions may be due to the fluorescence of retained basal laminar deposit (BLamD) detected by the Spectralis. We also found that the qAF in non-GA macular regions is much lower than in normal control eyes [20], suggesting poor macular health generally, consistent with the lower qAF measured in AMD histopathology [21]. This reinforces AMD pathophysiology: loss of LF, not an increase, marks progression.

Anatomically, GA in the SDD pathway tends to be multilobular and extrafoveal (consistent with our previous results [6], which also found new GA appearing preferentially in areas with SDD [22]) and that in the drusen pathway more isolated and central, as also observed by Mones et al [14]. However, the pathways are not mutually exclusive and may even be confluent, as was seen in 10 of 23 of eyes. This further complexity may explain why the two fundamental pathways have not been previously suggested as distinct entities.

The two distinct pathways suggest different disease mechanisms, to be determined, driving the formation and progression of the two iAMD lesions. Thomson et al have just reported a strong connection of SDDs, not drusen, to CVD and stroke, consistent with a vascular mechanism [23]. They also report additional data from genetics and serum risks that support the two-disease hypothesis [23]. Slower AMD progression after laser treatment in drusen eyes and exacerbation in SDD eyes suggests fundamentally different pathobiology [24, 25]. Soft drusen correlate spatially with cone photoreceptors centrally, and SDD with the rods peripherally [26], suggesting different photoreceptor-specific process. SDD have also been associated with choroidal thinning [27, 28], and choriocapillaris insufficiency [29, 30]. In one study, SFCT in patients with SDD was less than half that seen with drusen [31], all suggesting a choroidal role in GA arising from SDD. In this study, at baseline, there was significantly thinner mean SFCT in eyes with SDD, with or without drusen, than in the eyes with only drusen, but not at final follow-up, perhaps due to choroidal thinning with development of GA and with age in all patients

The source of higher qAF in SDD-associated GA we posit to be BLamD, following the original suggestion specifically regarding "gray" GA in the diffuse tricking AF phenotype [12]. In the near absence of the RPE and its lipofuscin, as well as the iAMD precursors themselves, other fluorescent structures become candidates. The remaining layers of BrM and the inner retina are intact in each and would contribute equally. The most likely AF source, then, in the absence of drusen, would be BLamD. BLamD and drusen spectral characteristics have been studied ex vivo [32]. Their shorter wavelength emissions, peaking near 520 nm, would still pass the 500 nm emission filter of the Spectralis. Residual BLamD has been described histologically and may be seen on SD-OCT as plateaus and splits in RPE/BrM in advanced AMD. The high prevalence (80%) of BLamD containing structures in B-scans through SDD-associated GA (Figs. 2 and 3) relative to drusen-associated GA (4%) (Fig. 1) found herein may be responsible for the higher qAF signal in SDD-associated atrophy. Significantly, only minimal retained RPE was found in SDD-associated GA, further confirming that the source of this higher qAF is BLamD.

Preservation of BLamD with drusen regression is also described [19]. Other presentations of persistent BLamD in geographic atrophy are outer retinal corrugations and "wedge" [9, 19, 33, 34].

BLamD has recently been reported in the pathology of extensive macular atrophy with pseudodrusen, again tying SDD to BLamD [35]. To our knowledge, ours is the first description of a strong general association of SDD versus drusen with BLamD. Direct histopathologic correlation is warranted.

This study has several limitations. First, the sample size was small, so all conclusions must be considered speculative, pending further research. The small size was partly because of our strict inclusion criteria: pseudophakic patients with clear posterior capsule to avoid confounding lens effects on qAF. However, there are other possible biologic confounders such as absorption of the excitation light by incompletely bleached photopigment [16]. The time an atrophic lesion exists might also affect its qAF. Thus, the differences in qAF that we observed might not persist over years of follow-up.

A strength of the study is the very consistent finding of higher mean qAF in SDD-associated GA lesions than in drusen associated lesions, with intermediate mean qAF in GA with mixed precursors. Thus, a single objective metric, qAF, provides simplifying diagnostic information about an otherwise complex process that should be helpful to CAM efforts to identify precursors to atrophy, particularly for inferring the history of an eye which is otherwise absent. Higher qAF was also strongly correlated with OCT imaging markers for retained BLamD in SDD-associated GA, suggesting that this BLamD is not only the source of the higher qAF in these lesions, but is related to SDD mechanism.

In conclusion, there are potentially two different pathways to GA that are associated with the two characteristic iAMD phenotypes of drusen and SDD, and that can be differentiated by the surrogate marker of quantitative autofluorescence (qAF) in their outcomes. The source of the greater autofluorescence in SDD-associated GA appears to be basal laminar deposit (BLamD). All these conclusions are provisional, pending replication in larger studies, but are of high significance. Quantitative autofluorescence and individual consideration of the two SDD- and drusen-associated pathways might improve the interpretation of research on GA mechanisms, treatments and prognostic factors for disease progression.

SUMMARY

What was known before

- Geographic atrophy (GA) is the atrophic advanced form of age-related macular degeneration (AMD).
- The mechanism of progression to GA is unknown.

What this study adds

- GA appears to proceed along two distinct pathways, originating from drusen and subretinal drusenoid deposits (SDDs), respectively, with distinct imaging characteristics on quantitative autofluorescence.
- Structurally, SDD-associated lesions, in contrast to drusen-associate lesions, are specifically accompanied by basal laminar deposit, suggesting two separate mechanisms to be explored.

DATA AVAILABILITY

The datasets generated during and/or analysed during the current study are available from the corresponding author on reasonable request.

REFERENCES

1. Sadda SR, Guymer R, Holz FG, Schmitz-Valckenberg S, Curcio CA, Bird AC, et al. Consensus definition for atrophy associated with age-related macular degeneration on OCT: classification of atrophy report 3. Ophthalmology. 2018;125:537–48.
2. Oak AS, Messinger JD, Curcio CA. Subretinal drusenoid deposits: further characterization by lipid histochemistry. Retina. 2014;34:825–6.
3. Zweifel SA, Spaide RF, Curcio CA, Malek G, Imamura Y. Reticular pseudodrusen are subretinal drusenoid deposits. Ophthalmology. 2010;117:303–12.e1.
4. Klein R, Meuer SM, Knudtson MD, Iyengar SK, Klein BE. The epidemiology of retinal reticular drusen. Am J Ophthalmol. 2008;145:317–26.
5. Pumariega NM, Smith RT, Sohrab MA, LeTien V, Souied EH. A prospective study of reticular macular disease. Ophthalmology. 2011;118:1619–25.
6. Xu L, Blonska AM, Pumariega NM, Bearelly S, Sohrab MA, Hageman GS, et al. Reticular macular disease is associated with multilobular geographic atrophy in age-related macular degeneration. Retina. 2013;33:1850–62.
7. Nagiel A, Sarraf D, Sadda SR, Spaide RF, Jung JJ, Bhavsar KV, et al. Type 3 neovascularization: evolution, association with pigment epithelial detachment, and treatment response as revealed by spectral domain optical coherence tomography. Retina. 2015;35:638–47.
8. Smith RT, Merriam JE, Sohrab MA, Pumariega NM, Barile G, Blonska AM, et al. Complement factor H 402H variant and reticular macular disease. Arch Ophthalmol. 2011;129:1061–6.
9. Tong YAT, Curcio C, Smith RT. Hyperspectral autofluorescence characterization of drusen and sub-RPE deposits in age-related macular degeneration. Ann Eye Sci. 2021;6:4.
10. Schmitz-Valckenberg S, Sahel J-A, Danis R, Fleckenstein M, Jaffe GJ, Wolf S, et al. Natural history of geographic atrophy progression secondary to age-related macular degeneration (Geographic Atrophy Progression Study). Ophthalmology. 2016;123:361–8.
11. Biarnes M, Arias L, Alonso J, Garcia M, Hijano M, Rodriguez A, et al. Increased fundus autofluorescence and progression of geographic atrophy secondary to age-related macular degeneration: the GAIN study. Am J Ophthalmol. 2015;160:345–53.e5.
12. Fleckenstein M, Schmitz-Valckenberg S, Martens C, Kosanetzky S, Brinkmann CK, Hageman GS, et al. Fundus autofluorescence and spectral-domain optical coherence tomography characteristics in a rapidly progressing form of geographic atrophy. Investigative Ophthalmol Vis Sci. 2011;52:3761–6.
13. Fleckenstein M, Schmitz-Valckenberg S, Lindner M, Bezatis A, Becker E, Fimmers R, et al. The "diffuse-trickling" fundus autofluorescence phenotype in geographic atrophy. Invest Ophthalmol Vis Sci. 2014;55:2911–20.
14. Monés J, Biarnés M. Geographic atrophy phenotype identification by cluster analysis. Br J Ophthalmol. 2017;102:388–92.
15. Biarnes M, Colijn JM, Sousa J, Ferraro LL, Garcia M, Verzijden T, et al. Genotype and phenotype-based subgroups in geographic atrophy secondary to age-related macular degeneration. The EYE-RISK Consortium. Ophthalmol Retina. 2020;4:1129–37.
16. Delori F, Greenberg JP, Woods RL, Fischer J, Duncker T, Sparrow J, et al. Quantitative measurements of autofluorescence with the scanning laser ophthalmoscope. Invest Ophthalmol Vis Sci. 2011;52:9379–90.
17. Armenti ST, Greenberg JP, Smith RT. Quantitative fundus autofluorescence for the evaluation of retinal diseases. J Vis Exp. 2016;11:53577.
18. Demirkaya N, van Dijk HW, van Schuppen SM, Abràmoff MD, Garvin MK, Sonka M, et al. Effect of age on individual retinal layer thickness in normal eyes as measured with spectral-domain optical coherence tomography. Investigative Opthalmology Vis Sci. 2013;54:4934.
19. Sura AA, Chen L, Messinger JD, Swain TA, McGwin G Jr., Freund KB, et al. Measuring the contributions of basal laminar deposit and Bruch's membrane in age-related macular degeneration. Invest Ophthalmol Vis Sci. 2020;61:19.
20. Orellana-Rios J, Yokoyama S, Agee JM, Challa N, Freund KB, Yannuzzi LA, et al. Quantitative fundus autofluorescence in non-neovascular age-related macular degeneration. Ophthalmic Surg Lasers Imaging Retin. 2018;49:S34–42.
21. Ach T, Tolstik E, Messinger JD, Zarubina AV, Heintzmann R, Curcio CA. Lipofuscin redistribution and loss accompanied by cytoskeletal stress in retinal pigment epithelium of eyes with age-related macular degeneration. Invest Ophthalmol Vis Sci. 2015;56:3242–52.
22. Marsiglia M, Boddu S, Bearelly S, Xu L, Breaux BE Jr., Freund KB, et al. Association between geographic atrophy progression and reticular pseudodrusen in eyes with dry age-related macular degeneration. Invest Ophthalmol Vis Sci. 2013;54:7362–9.
23. Thomson RJ, Chazaro J, Otero-Marquez O, Ledesma-Gil G, Tong Y, Coughlin AC, et al. Subretinal drusenoid deposits and soft drusen: are they markers for distinct retinal diseases? Retina. 2022;42:1311–8.
24. Guymer RH, Wu Z, Hodgson LAB, Caruso E, Brassington KH, Tindill N, et al. Subthreshold nanosecond laser intervention in age-related macular

degeneration: the LEAD randomized controlled clinical trial. Ophthalmology. 2019;126:829–38.
25. Theodore Smith R. Sub-threshold nanosecond laser (SNL) treatment in intermediate AMD (IAMD). Ann Eye Sci. 2019;4:2.
26. Curcio CA, Sloan KR, Kalina RE, Hendrickson AE. Human photoreceptor topography. J Comp Neurol. 1990;292:497–523.
27. Cheng H, Kaszubski PA, Hao H, Saade C, Cunningham C, Freund KB, et al. The relationship between reticular macular disease and choroidal thickness. Curr eye Res. 2016;41:1492–7.
28. Garg A, Oll M, Yzer S, Chang S, Barile GR, Merriam JC, et al. Reticular pseudodrusen in early age-related macular degeneration are associated with choroidal thinning. Invest Ophthalmol Vis Sci. 2013;54:7075–81.
29. Lains I, Wang J, Providencia J, Mach S, Gil P, Gil J, et al. Choroidal changes associated with subretinal drusenoid deposits in age-related macular degeneration using swept-source optical coherence tomography. Am J Ophthalmol. 2017;180:55–63.
30. Nesper PL, Soetikno BT, Fawzi AA. Choriocapillaris nonperfusion is associated with poor visual acuity in eyes with reticular pseudodrusen. Am J Ophthalmol. 2017;174:42–55.
31. Switzer DW Jr., Mendonca LS, Saito M, Zweifel SA, Spaide RF. Segregation of ophthalmoscopic characteristics according to choroidal thickness in patients with early age-related macular degeneration. Retina. 2012;32:1265–71.
32. Tong Y, Ami TB, Hong S, Heintzmann R, Gerig G, Ablonczy Z. et al. Hyperspectral autofluorescence imaging of drusen and retinal pigment epithelium in donor eyes with age-related macular degeneration. Retina (Philadelphia. Pa). 2016;36:S127–36.
33. Tan ACS, Astroz P, Dansingani KK, Slakter JS, Yannuzzi LA, Curcio CA, et al. The evolution of the plateau, an optical coherence tomography signature seen in geographic atrophy. Investigative Ophthalmol Vis Sci. 2017;58:2349–58.
34. Querques G, Capuano V, Frascio P, Zweifel S, Georges A, Souied EH. Wedge-shaped subretinal hyporeflectivity in geographic atrophy. Retina. 2015;35:1735–42.
35. Fragiotta S, Parravano M, Sacconi R, Costanzo E, Viggiano P, Prascina F, et al. A Common Finding in Foveal-Sparing Extensive Macular Atrophy with Pseudodrusen Implicates Basal Laminar Deposits. Retina. 2022;42:1319–29.

AUTHOR CONTRIBUTIONS

WW: acquisition of data, analysis and interpretation of data, manuscript preparation MM: acquisition of data, analysis and interpretation of data, manuscript preparation. OOM: analysis and interpretation of data, manuscript preparation. YT: analysis and interpretation of data, manuscript preparation. ES: analysis and interpretation of data, manuscript preparation. GQ: analysis and interpretation of data, manuscript preparation. KBF: design, acquisition of data, analysis and interpretation of data, manuscript preparation. RTS: design, acquisition of data, analysis and interpretation of data, manuscript preparation.

FUNDING

NIH R01 EY015520 (RTS), Macula Foundation (KBF). The sponsor or funding organization had no role in the design or conduct of this research.

COMPETING INTERESTS

The authors declare no competing interests.

ADDITIONAL INFORMATION

Correspondence and requests for materials should be addressed to R. Theodore Smith.